Journal of Discrete Mathematics and Its Applications 9 (4) (2024) 269–287

Journal of Discrete Mathematics and Its Applications

Available Online at: http://jdma.sru.ac.ir

*Research Paper*

# A combined efficient method for approximating the solution of two-dimensional integral equations

**Mohsen Fallahpour***, **Reza Ezzati, Elham Hashemizadeh**

Department of Mathematics, Karaj Branch, Islamic Azad University, Karaj, I. R. Iran

**Academic Editor:** Vahid Mohammadi

**Abstract.** In this paper, we combine the two-dimensional (2D) Haar wavelet functions (HWFs) with the block-pulse functions (BPFs) to solve the 2D linear Volterra-Fredholm integral equations (2D-L(VF)IE). This approach presents a new hybrid computational effcient method based on the 2D-HWFs and 2D-BPFs to approximate the solution of the 2D linear Volterra-Fredholm integral equations. In fact, the HWFs and their relations to the BPFs are employed to derive a general procedure to form operational matrix of Haar wavelets. Theoretical error analysis of the proposed method is done. Finally some examples are presented to show the effectiveness of the proposed method.

**Keywords.** Haar wavelet, block-pulse functions, operational matrix, two-dimensional integral.
**Mathematics Subject Classification (2020):** $65C20$, $45Axx$, $45Bxx$, $45Dxx$, $65T60$.

## 1 Introduction

As we know, the 2D-L(VF)IEs appear in various fields of scienc and engineering, such as heat conduction, concrete mechanics, electroelastics, contact phisics and plasma physics. To solve these equations, we encounter computational intricacies. We can see some numerical

*Corresponding author (Email address: M.Fallahpour@kiau.ac.ir).
Received 18 October 2024; Revised 07 November 2024 ; Accepted 23 November 2024
First Publish Date: 01 December 2024

 

methods for solving such equations in [5–18]. In this work we consider the equation

$$g(x,y) = f(x,y) + \int_0^1 \int_0^1 c_1(x,y,s,t)g(s,t)dsdt \\ + \int_0^y \int_0^x c_2(x,y,s,t)g(s,t)dsdt, \tag{1}$$

where $(x,y) \in [0,1]^2$. Also $f$ and the kernels $c_1$, $c_2$ in Eq. (1) are the known functions and $g$ is the unknown function such that the functions $f$ and $g$ are defined in the space $L^2[0,1]$ and the functions $c_1$ and $c_2$ are defined in the space $L^4[0,1]$.

In this work, we use the presented method of [1] to obtain the numerical solution of Eq. (1) based on the HWFs and their relations to the BPFs.

The structure of this paper is as follows: In Section 2, we present some basic properties about 2D-BPFs and 2D-HWFs. Also, we introduce a general procedure for deriving the operational matrix of Haar wavelets by using relations between the HWFs and BPFs. In Section 3, we apply this operational matrices for solving the 2D-L(VF)IE in Eq. (1). In Section 4, the theorems are provided for the convergence analysis. In Section 5, we apply the proposed method in some numerical examples. Finally, a conclusion is given in Section 6.

## 2 Preliminaries

In this section, we examine some basic concepts about HWFs and BPFs and their relationships with each other.

### 2.1 Block-pulse functions

An $n$-set of the BPFs $b_a(x)$ are as [2]

$$b_a(x) = \begin{cases} 1 & (a-1)k \leq x < ak \\ 0 & otherwise \end{cases}$$

where $x \in [0,T)$, $a = 1,2,\ldots,n$ and $k = \dfrac{T}{n}$.

We can write every square integrable function $f(x)$ as

$$f(x) \simeq \sum_{a=1}^{n} f_a b_a(x), \tag{2}$$

where $b_i(x)$ are the entries of the BPFs vector $B(x) = [b_1(x), b_2(x), ..., b_n(x)]^T$, and for $a = 1,2,...,n$

$$f_a = \frac{1}{k}\int_0^T b_a(x) f(x) dx.$$

From Eq. (2) we have

$$f(x) \simeq F^T B(x) = B^T(x) F,$$

in which $F=[f_1,f_2,...,f_n]^T$. Moreover, for every 2D function $c(x,y)\in L^2([0,T_1)\times[0,T_2))$ we have

$$c(x,y)=C^TB(x,y)=B^T(x)CB(y),$$

where here $C_{n\times n}$ is the BPFs coefficient matrix with

$$c_{ij}=\frac{1}{k_1k_2}\int_0^{T_1}\int_0^{T_2}c(x,y)b_i(x)b_j(y)dxdy,$$

for $i,j=1,2,...,n$, where $k_1=\frac{T_1}{n}$, $k_2=\frac{T_2}{n}$ and $B(x,y)$ is the block-pulse vector defined by

$$B=[b_{1,1},b_{1,2},...,b_{n,n}]^T. \tag{3}$$

We have

$$\int_0^x B(s)ds\simeq PB(x),$$

where $P_{n\times n}$ is

$$P=\frac{k}{2}\begin{pmatrix}1&2&2&\dots&2\\0&1&2&\dots&2\\0&0&1&\dots&2\\\vdots&\vdots&\vdots&\ddots&\vdots\\0&0&0&\dots&1\end{pmatrix}, \tag{4}$$

and the integral of vector $B(x)$ is obtained as

$$\int_0^1 B(s)ds\simeq D,$$

where $D_{n\times n}$ is

$$D=\begin{pmatrix}k&0&\dots&0\\0&k&\dots&0\\\vdots&\vdots&\ddots&\vdots\\0&0&\dots&k\end{pmatrix}. \tag{5}$$

### 2.2 Haar wavelets

We know that the mathematical formula of HWFs $(\psi_{j,k}(y))_{j\in N,k\in Z}$, is as [4]

$$\psi_{j,k}(y)=2^{j/2}h\left(2^jy-k\right)\ ,\ j\geq 0\ ,\ 0\leq k<2^j\ ,\ j,k\in Z,$$

such that for $h_i(y)$ in the support $[\frac{k}{2^j},\frac{k+1}{2^j})$, on $[0,1)$, we have some important properties

$$h_1(y)=\begin{cases}1, for\ \mathrm{y}\in[0,1)\\0,\ \ otherwise\end{cases}$$

$$h_i(y) = \begin{cases} 1 & for \text{ y} \in [\alpha_i, \beta_i) \\ -1, & for \text{ y} \in [\beta_i, \gamma_i) \\ 0, & otherwise, \quad i = 2, 3, ... \end{cases}$$

$$\alpha_i = \frac{i}{n}, \quad \beta_i = \frac{(i + 0.5)}{n}, \quad \gamma_i = \frac{(i + 1)}{n};$$
$$n = 2^\ell, \quad \ell = 0, 1, ..., \quad i = 0, 1, ..., n - 1.$$

So for the integrable function $f(x)$ we have

$$f(x) \simeq f_1 h_1(x) + \sum_{i=1}^{n-1} f_i h_i(x),\ i = 2^j + k,\ j = 0, 1, ..., J - 1,\ 0 \leq k < 2^j. \tag{6}$$

From Eq. (6) we can get

$$f \simeq F^T H = H^T F,$$

where

$$F = [f_1, f_2, ..., f_n]^T,$$
$$H = [h_1, h_2, ..., h_n]^T. \tag{7}$$

Also, any 2D function $c(x, y)$ can be expanded with respect to the HWFs as

$$c(x, y) = C^T H(x, y) = H^T(x, y)C = H^T(x)CH(y),$$

where $C$ is the $n^2 \times n^2$ Haar wavelet with

$$c_{ij} = \int_0^1 \int_0^1 c(x, y) h_i(x) h_j(y) dx dy, \quad i, j = 1, 2, ..., n,$$

and $H(x, y)$ is the wavelet vector as

$$H = [h_{1,1}, h_{1,2}, ..., h_{n,n}]^T. \tag{8}$$

### 2.3 Relations between BPFs and HWFs

We set $T = 1$ defined in Section 2.1. If we consider $H(x)$ and $B(x)$ as the n-dimensional HWFs and BPFs vectors, respectively, we have from [1] that

$$H(x) = QB(x), \tag{9}$$

with

$$Q_{n\times n} = [Q_{ij}]_{n\times n} = 2^{(j\backslash 2)} h_{i-1}(\frac{2j - 1}{2n}), \tag{10}$$

for $n = 2^J$, $i, j = 1, 2, ..., n$, $i - 1 = 2^j + k$ and $0 \leq k < 2^j$. Here we desire a formula similar to Eq. (9) in the 2D case. To do this, by using the 2D-BPFs, 2D-HWFs and Eq. (9) we can obtain

$$H(x,y) = RB(x,y), \tag{11}$$

where

$$R_{n^2 \times n^2} = Q_{n \times n} \otimes Q'_{n \times n}, \tag{12}$$

and $\otimes$ denotes the Kronecker product. Now we have

$$H(x)H^T(x)F = \tilde{F}H(x),$$

where

$$\tilde{F}_{n \times n} = Q\bar{F}Q^{-1}, \tag{13}$$

and

$$\bar{F} = diag(Q^T F).$$

Similarly we can write

$$H(x,y)H^T(x,y)E_{n \times n} = \tilde{E}H(x,y), \tag{14}$$

where

$$\tilde{E}_{n^2 \times n^2} = \tilde{F}_{n \times n} \otimes \tilde{F}'_{n \times n}.$$

Also for the arbitrary matrix $M$ we have

$$H^T(x)MH(x) = \hat{M}^T H(x),$$

where $\hat{M} = UQ^{-1}$ and $U = diag(Q^T MQ)$ is an $n-$vector. Similarly for an arbitrary $n^2 \times n^2$ matrix we obtain

$$H^T(x,y)LH(x,y) = \hat{L}^T H(x,y), \tag{15}$$

where

$$\hat{L} = SR^{-1},$$

and $S = diag(R^T LR)$ is a $(n \times n)-$vector and $R$ is introduced in Eq. (12).

### 2.4 Operational matrix of HWFs

In this subsection, we obtain the integration operational matrix for the HWFs. Suppose $H(x)$ is the HWFs vector defined in Eq. (7). The integral of this vector can be derived as [1]

$$\int_0^x H(s)ds \simeq \frac{1}{n}QPQ^T H(x) = \Lambda H(x). \tag{16}$$

where $Q$ is introduced in Eq. (10) and $P$ is the operational matrix of integration for the BPFs derived in Eq. (4). The following remarks are the consequence of the HWFs and the BPFs properties.

**Remark 2.1.** *Suppose $H(x,y)$ is the HWFs vector defined in Eq.* (8)*. Then*

$$\int_0^1 \int_0^1 H^T(s,t)H(s,t)dsdt \simeq ROR^T = A_1,$$

*where $O_{n^2 \times n^2}$ is as $D \otimes D$ in which $D$ is the operational matrix of integration for the BPFs derived in Eq.* (5)*.*

**Remark 2.2.** *For the 2D-Volterra integral of vector $H(x,y)$ we have*

$$\int_0^y \int_0^x H(s,t)dsdt \simeq (\Lambda \otimes \Lambda)_{n^2 \times n^2} H(x,y) = A_2 H(x,y),$$

*where $\Lambda$ is derived from Eq.* (16)*.*

## 3 Solving 2D-L(VF)IE

In this section, we approximate $g$, $f$, $c_1$ and $c_2$ in terms of the HWFs as

$$g(x,y) = G^T H(x,y), \tag{17}$$

$$f(x,y) = F^T H(x,y), \tag{18}$$

$$c_1(x,y,s,t) = C_1^T H(x,y,s,t) = H^T(x,y) C_1 H(s,t), \tag{19}$$

and

$$c_2(x,y,s,t) = C_2^T H(x,y,s,t) = H^T(x,y) C_2 H(s,t), \tag{20}$$

where $G$, $F$, $C_1$ and $C_2$ are the HWFs coefficients of $g$, $f$, $c_1$ and $c_2$, respectively, and $H$ is defined in Eq. (8). In Eq. (18), $F$ is the $(n_1 n_2 \times 1)$ known vector, also in Eqs. (19) and (20), $C_1$ and $C_2$ are the $(n_1 n_2) \times (n_1 n_2)$ known matrices but in Eq. (17), $G$ is the $(n_1 n_2 \times 1)$ unknown vector.
By using Eqs. (17), (19) and Remark 2.1 we get

$$\begin{aligned}\int_0^1 \int_0^1 c_1(x,y,s,t) g(s,t) dsdt &= \int_0^1 \int_0^1 H^T(x,y) C_1 H(s,t) H^T(s,t) G dsdt \\ &= H^T(x,y) C_1 \left( \int_0^1 \int_0^1 H(s,t) H^T(s,t) dsdt \right) G \\ &= H^T(x,y) C_1 A_1 G = (C_1 A_1 G)^T H(x,y) = \hat{G}_F^T H(x,y),\end{aligned}$$

where $\hat{G}_F^T$ is an $(n^2 \times n^2)$-vector obtained as $C_1 A_1 G$. So we have

$$\int_0^1 \int_0^1 c_1(x,y,s,t) g(s,t) dsdt \simeq \hat{G}_F^T H(x,y). \tag{21}$$

Also by Eqs. (14), (17) and (20), we get

$$\begin{aligned}\int_0^y\int_0^x c_2(x,y,s,t)g(s,t)dsdt &\simeq \int_0^y\int_0^x H^T(x,y)C_2H(s,t)H^T(s,t)Gdsdt\\ &= H^T(x,y)C_2\left(\int_0^y\int_0^x H(s,t)H^T(s,t)Gdsdt\right)\\ &= H^T(x,y)C_2\left(\int_0^y\int_0^x \tilde{G}H(s,t)dsdt\right)\\ &= H^T(x,y)C_2\tilde{G}\left(\int_0^y\int_0^x H(s,t)dsdt\right).\end{aligned}$$

Now, from Remark 2.2, we have

$$\int_0^y\int_0^x c_2(x,y,s,t)g(s,t)dsdt \simeq H^T(x,y)C_2\tilde{G}A_2H(x,y),$$

in which $C_2\tilde{G}A_2$ is an $(n_1n_2)\times(n_1n_2)$ matrix. So we conclude that

$$\int_0^y\int_0^x c_2(x,y,s,t)g(s,t)dsdt \simeq \hat{G}_V^TH(x,y), \tag{22}$$

where $\hat{G}_V^T$ is an $(n_1n_2)$-vector.
Applying Eqs. (17), (18), (21) and (22) in Eq. (1), we get

$$F^TH + \hat{G}_F^TH + \hat{G}_V^TH. \tag{23}$$

Replacing $\simeq$ with $=$, Eq. (23) gives

$$G - \hat{G}_F - \hat{G}_V = F. \tag{24}$$

Equation (24) generates a system of the $(n_1n_2)$ linear equations with the $(n_1n_2)$ unknown variable. Clearly, we can solve Eq. (24) using either direct methods or iterative methods, the latter of which may include Newton's method.

## 4 Convergence analysis

In this section, we investigate the convergence of the current method for solving Eq. (1).
At first, we consider the 2−norms defined in this paper as:
If $f\in C[a,b]$, $g\in C([a_1,b_1]\times[a_2,b_2])$ and $c\in C([a_1,b_1]\times[a_2,b_2]\times([a_3,b_3]\times[a_4,b_4])$, we can define a 2−norm by

$$\|f\| = \|f\|_2 = \left[\int_a^b |f(x)|^2dx\right]^{\frac{1}{2}},$$

$$\|g\| = \|g\|_2 = \left[\int_{a_1}^{b_1}\int_{a_2}^{b_2} |g(x,y)|^2dxdy\right]^{\frac{1}{2}}$$

and

$$\|c\| = \|c\|_2 = \left[ \int_{a_1}^{b_1} \int_{a_2}^{b_2} \int_{a_3}^{b_3} \int_{a_4}^{b_4} |c(x,y,s,t)|^2 dxdydsdt \right]^{\frac{1}{2}}.$$

Also we know that for a differentiable function $u$ with a bounded derivative, there is a real number $M$ such that [3]

$$|u(s) - u(t)| \leq M|s - t|. \tag{25}$$

**Theorem 4.1.** *For function $c \in L^4([0,1))$ with*

$$|\frac{\partial^4 c}{\partial x \partial y \partial s \partial t}| \leq V,$$

*where $V$ is the upper bound for the fourth-order derivative of function $c(x,y,s,t)$ and the 4D Haar wavelet expansion of $c$ as*

$$\hat{c}_n(x,y,s,t) = \sum_{p=0}^{n-1} \sum_{q=0}^{n-1} \sum_{r=0}^{n-1} \sum_{l=0}^{n-1} c_{pqrl} h_p(x) h_q(y) h_r(s) h_l(t),$$

*the reperesentation error between $c$ and $\hat{c}_n$ is as*

$$\|e_{p,q,r,l}\| \leq \frac{V}{9n^4},$$

*where*

$$e_{p,q,r,l} = c - \hat{c}_n.$$

*Proof.* By the error definition we can write

$$\begin{aligned}
\|e_{p,q,r,l}\|^2 &= \int_0^1 \int_0^1 \int_0^1 \int_0^1 \left( c(x,y,s,t) - \sum_{p=0}^{n-1} \sum_{q=0}^{n-1} \sum_{r=0}^{n-1} \sum_{l=0}^{n-1} c_{pqrl} h_p(x) h_q(y) h_r(s) h_l(t) \right)^2 dtdsdydx \\
&= \int_0^1 \int_0^1 \int_0^1 \int_0^1 \left( \sum_{p=n}^{\infty} \sum_{q=n}^{\infty} \sum_{r=n}^{\infty} \sum_{l=n}^{\infty} c_{pqrl} h_p(x) h_q(y) h_r(s) h_l(t) \right)^2 dtdsdydx \\
&= \sum_{p=n}^{\infty} \sum_{q=n}^{\infty} \sum_{r=n}^{\infty} \sum_{l=n}^{\infty} c_{pqrl}^2,
\end{aligned} \tag{26}$$

where $p = 2^{j_1} + k$, $q = 2^{j_2} + k$, $r = 2^{j_3} + k$, $l = 2^{j_4} + k$, $n = 2^J$, $J > 0$ and

$$c_{pqrl} = \int_0^1 \int_0^1 \int_0^1 \int_0^1 h_p(x) h_q(y) h_r(s) h_l(t) c(x,y,s,t) dtdsdydx.$$

Based on the HWFs definition, mean value theorem, Eq. (25) and [1, Theorem 5], there are $\eta_{j_4}, \alpha, \alpha', \eta_{j_3}, \beta, \beta', \eta_{j_2}, \gamma, \gamma', \eta_{j_1}, \theta, \theta'$, that

$$\alpha, \alpha' \in [k2^{-j_4}, (k + \frac{1}{2})2^{-j_4}] \ , \ \beta, \beta' \in [k2^{-j_3}, (k + \frac{1}{2})2^{-j_3}],$$

$$\gamma,\gamma' \in [k2^{-j_2},(k+\frac{1}{2})2^{-j_2}] \ \ , \ \ \theta,\theta' \in [k2^{-j_1},(k+\frac{1}{2})2^{-j_1}],$$

such that

$$\begin{aligned}
c_{pqrl} &= \int_0^1\int_0^1\int_0^1 h_p(x)h_q(y)h_r(s)\times\left(\int_0^1 h_l(t)c(x,y,s,t)dt\right)dsdydx\\
&= \int_0^1\int_0^1\int_0^1 h_p(x)h_q(y)h_r(s)\times\left(2^{(\frac{-j_4}{2}-1)}(\alpha-\alpha')\frac{\partial c(x,y,s,\eta_{j_4})}{\partial t}\right)dsdydx\\
&= \int_0^1\int_0^1 h_p(x)h_q(y)\times 2^{\left(\frac{-j_4}{2}-1\right)}(\alpha-\alpha')\times\left(\int_0^1 h_r(s)\frac{\partial c(x,y,s,\eta_{j_4})}{\partial t}ds\right)dydx\\
&= \int_0^1\int_0^1 2^{\left(\frac{-j_4}{2}-\frac{-j_3}{2}-2\right)}\times(\alpha-\alpha')\times(\beta-\beta')\frac{\partial^2 c(x,y,\eta_{j_3},\eta_{j_4})}{\partial s\partial t}h_p(x)h_q(y)dydx.
\end{aligned}$$

Similarly we get

$$c_{pqrl} = 2^{(\frac{-j_4}{2}-\frac{-j_3}{2}-\frac{-j_2}{2}-\frac{-j_1}{2}-4)}\times(\alpha-\alpha')(\beta-\beta')\times(\gamma-\gamma')(\theta-\theta')\frac{\partial^4 c(\eta_{j_1},\eta_{j_2},\eta_{j_3},\eta_{j_4})}{\partial x\partial y\partial s\partial t}.$$

Also from Eq. (26) we have

$$\begin{aligned}
\|e_{p,q,r,l}\|^2 &= \sum_{p=n}^{\infty}\sum_{q=n}^{\infty}\sum_{r=n}^{\infty}\sum_{l=n}^{\infty}2^{(-j_4-j_3-j_2-j_1-8)}\\
&\quad\times(\alpha-\alpha')^2(\beta-\beta')^2(\gamma-\gamma')^2(\theta-\theta')^2\left|\frac{\partial^4 K(\eta_{j_1},\eta_{j_2},\eta_{j_3},\eta_{j_4})}{\partial x\partial y\partial s\partial t}\right|^2\\
&\le \sum_{p=n}^{\infty}\sum_{q=n}^{\infty}\sum_{r=n}^{\infty}\sum_{l=n}^{\infty}2^{(-j_4-j_3-j_2-j_1-8)}\times 2^{-2j_1}\times 2^{-2j_2}\times 2^{-2j_3}\times 2^{-2j_4}\times V^2\\
&= \sum_{p=n}^{\infty}\sum_{q=n}^{\infty}\sum_{r=n}^{\infty}\sum_{l=n}^{\infty}2^{(-3j_4-3j_3-3j_2-3j_1-8)}\times V^2\\
&= V^2\sum_{p=n}^{\infty}\sum_{q=n}^{\infty}2^{(-3j_2-3j_1-4)}\sum_{r=n}^{\infty}\sum_{l=n}^{\infty}2^{(-3j_4-3j_3-4)},
\end{aligned}$$

therefore we can derive

$$\|e_{p,q,r,l}\|^2 \le V^2\times\frac{1}{9n^4}\times\frac{1}{9n^4} = \frac{V^2}{81n^8}.$$

In other words

$$\|e_{p,q,r,l}\| \le \frac{V}{9n^4}.$$

□

**Theorem 4.2.** *If $g(s,t)$ and $\hat{g}_n(s,t)$ are the exact and approximate solutions of Eq.* (1) *respectively, that are obtained by Eq.* (24) *with*

1. $\|g\| \leq Y$,
2. $\|c_i\| \leq W_i, \ \ i = 1,2$,
3. $|\frac{\partial^4 c_i}{\partial x \partial y \partial s \partial t}| \leq V_i, \ \ i = 1,2$,
4. $\left(W_1 + W_2 + \frac{V_1 + V_2}{9n^4}\right) < 1$,

*then*

$$\|g - \hat{g}_n\| \leq \frac{\frac{M}{3n^2} + \frac{V_1 Y}{9n^4} + \frac{V_2 Y}{9n^4}}{1 - \left[W_1 + W_2 + \frac{V_1 + V_2}{9n^4}\right]}.$$

*Proof.* From Eq. (1), we get

$$\begin{aligned} g(x,y) - \hat{g}_n(x,y) = f(x,y) - \hat{f}_n(x,y) & \\ + \int_0^1 \int_0^1 \left(c_1(x,y,s,t)g(s,t) - \hat{c}_{1,n}(x,y,s,t)\hat{g}_n(s,t)\right) dsdt & \\ + \int_0^y \int_0^x \left(c_2(x,y,s,t)g(s,t) - \hat{c}_{2,n}(x,y,s,t)\hat{g}_n(s,t)\right) dsdt, & \end{aligned}$$

then by mean value theorem for the 2D integrals we have

$$\|g - \hat{g}_n\| \leq \|f - \hat{f}_n\| + \|c_1 g - \hat{c}_{1,n}\hat{g}_n\| + xy\|c_2 g - \hat{c}_{2,n}\hat{g}_n\|. \tag{27}$$

From the first two conditions, Eq. (25) and Theorem 4.1 we have

$$\begin{aligned} \|c_1 g - \hat{c}_{1,n}\hat{g}_n\| &\leq \|c_1\|\|g - \hat{g}_n\| + \|c_1 - \hat{c}_{1,n}\| \left(\|g - \hat{g}_n\| + \|g\|\right) \\ &\leq W_1\|g - \hat{g}_n\| + \frac{V_1}{9n^4}\left(\|g - \hat{g}_n\| + Y\right) \\ &= \left(W_1 + \frac{V_1}{9n^4}\right)\|g(s,t) - \hat{g}_n(s,t)\| + \frac{V_1}{9n^4}Y. \end{aligned} \tag{28}$$

Similarly we have

$$\begin{aligned} \|c_2 g - \hat{c}_{2,n}\hat{g}_n\| &\leq \|c_2\|\|g - \hat{g}_n\| + \|c_2 - \hat{c}_{2,n}\| \left(\|g - \hat{g}_n\| + \|g\|\right) \\ &= \left(W_2 + \frac{V_2}{9n^4}\right)\|g(s,t) - \hat{g}_n(s,t)\| + \frac{V_2}{9n^4}Y. \end{aligned} \tag{29}$$

By substituting Eqs. (28) and (29) in Eq. (27) and using [1, Theorem 5] we can write

$$\begin{aligned} \|g - \hat{g}_n\| \leq \frac{M}{3n^2} &+ \left[\left(W_1 + \frac{V_1}{9n^4}\right)\|g - \hat{g}_n\| + \frac{V_1}{9n^4}Y\right] \\ &+ xy\left[\left(W_2 + \frac{V_2}{9n^4}\right)\|g - \hat{g}_n\| + \frac{V_2}{9n^4}Y\right]. \end{aligned}$$

By taking sup we have

$$\|g-\hat{g}_n\| \leq \frac{M}{3n^2} + \left[\left(W_1 + \frac{V_1}{9n^4}\right) \sup_{s\leq x\ ,\ t\leq y} \|g-\hat{g}_n\| + \frac{V_1}{9n^4}\Upsilon\right] + \sup_{x\in[0,1)} x \times \sup_{y\in[0,1)} y \left[\left(W_2 + \frac{V_2}{9n^4}\right) \sup_{s\leq x\ ,\ t\leq y} \|g-\hat{g}_n\| + \frac{V_2}{9n^4}\Upsilon\right],$$

so

$$\|g-\hat{g}_n\| \leq \frac{\dfrac{M}{3n^2} + \dfrac{V_1\Upsilon}{9n^4} + \dfrac{V_2\Upsilon}{9n^4}}{1-\left[W_1+W_2+\dfrac{V_1+V_2}{9n^4}\right]}.$$

Therefore using Hypothesis 4 we have

$$\|g-\hat{g}_n\| = O(\frac{1}{n^2}).$$ □

## 5 Numerical Examples

In this section, for the applicability of the proposed method, three numerical examples are given.

**Example 5.1.** *We consider*

$$g(x,y) = x + y - Sin(x) + \frac{Cos(y)}{2}(x^2y + xy^2) + \int_0^1\int_0^1 Sin(x)g(s,t)dsdt - \int_0^y\int_0^x Cos(y)g(s,t)dsdt$$

*with the exact solution*

$$g(x,y) = x + y.$$

*In Table 1 the absolute error ($e(x,y)$) and the minimum absolute error ($e_{min}$) for the arbitrary points are computed for the present method in the different values of J. According to Table 1, by applying the present method when J increases, $e(x,y)$ and $e_{min}$ decrease. You can see the 3D graphs of this example for $J=1$ in Fig. 1. Also in Table 2, the comparison of the computed results by the present method and the HWFs [18] and the BPFs [17] methods for Example 5.1 are shown. We see that the error in this method, compared to other methods is smaller.*

| $J$ | $e(0,0.21)$ | $e(0.12,0.32)$ | $e(0.11,0.76)$ | $e(0.51,0.51)$ | $e(0.79,0.81)$ | $e_{min}$ |
|---|---|---|---|---|---|---|
| 1 | 0.01948 | 0.05123 | 0.02350 | 0.68015 | 0.89125 | 0.0020 |
| 2 | 0.02031 | 0.06114 | 0.01551 | 0.68012 | 0.75049 | 0.0016 |
| 3 | 0.08949 | 0.01564 | 0.08159 | 0.68210 | 0.65020 | 0.0081 |
| 4 | 0.03636 | 0.09808 | 0.04660 | 0.54114 | 0.57585 | 0.0050 |
| 5 | 0.03802 | 0.09800 | 0.04528 | 0.12216 | 0.46025 | 0.0047 |
| 6 | 0.02996 | 0.08407 | 0.04480 | 0.10525 | 0.40755 | 0.0045 |

Table 1. $e(x,y)$ and $e_{min}$ of Example 1 for some valus of $J$.

| $(x,y)$ | $J$ | *Method* | $\bar{e}$ |
|---|---|---|---|
| $(0,0.21)$ | 2 | HWFs | 0.154601 |
| | | BPFs | 0.012645 |
| | | Current | 0.020311 |
| $(0.11,0.76)$ | | HWFs | 0.016133 |
| | | BPFs | 0.016701 |
| | | Current | 0.015519 |
| $(0,0.21)$ | 4 | HWFs | 0.036412 |
| | | BPFs | 0.036210 |
| | | Current | 0.036367 |
| $(0.11,0.76)$ | | HWFs | 0.170048 |
| | | BPFs | 0.045522 |
| | | Current | 0.046601 |

Table 2. Comparison of numerical results of current method with other methods in $J = 2,4$ for Example 5.1.

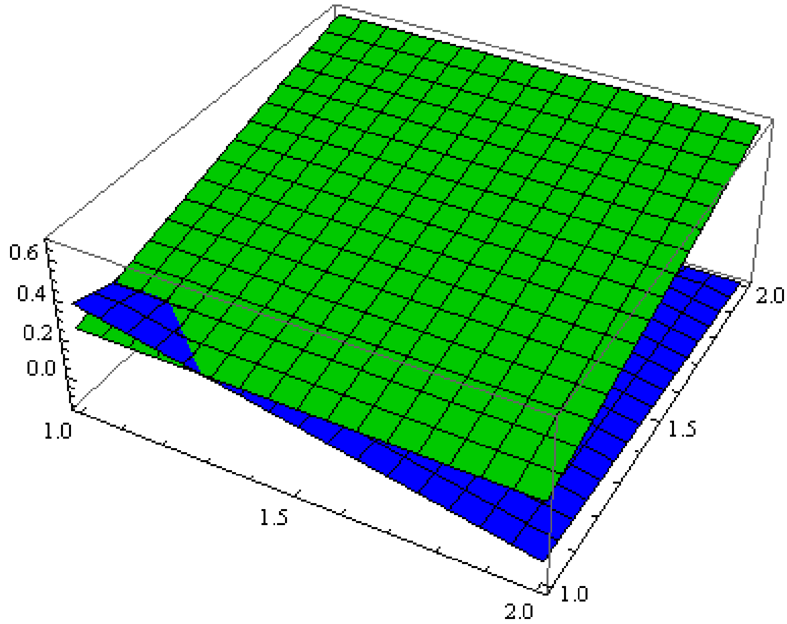


Figure 1. Exact and approximate solutions ($J = 1$) for Example 5.1.

**Example 5.2.** *We consider*

$$g(x,y) = Sin(x) + xy(Cos(1)+1) + y(Cos(1)-1) + \int_0^1\int_0^1 yg(s,t)dsdt - \int_0^y\int_0^x xg(s,t)dsdt,$$

*with the exact solution*

$$g(x,y) = Sin(x).$$

*In Table 2, $e(x,y)$ and $e_{min}$ for the arbitrary points are computed for the present method in the different values of $J$. According to Table 2, by applying this method when $J$ increases, $e(x,y)$ and $e_{min}$ decrease. You can see the 3D graphs of this example for $J = 3$ in Fig. 2. Also in Table 4, the comparison of the computed results by the present method and the HWFs [18] and the BPFs [17] methods for Example 5.2 are shown. We see that the error in this method, compared to other methods is smaller.*

| $J$ | $e(0,0.24)$ | $e(0.15,0.36)$ | $e(0.17,0.71)$ | $e(0.51,0.51)$ | $e(0.81,0.92)$ | $e_{min}$ |
|---|---|---|---|---|---|---|
| 1 | 0.10264 | 0.09112 | 0.04122 | 0.66510 | 0.91234 | 0.0065 |
| 2 | 0.08555 | 0.08414 | 0.09691 | 0.66415 | 0.90512 | 0.0265 |
| 3 | 0.04040 | 0.02390 | 0.03413 | 0.61234 | 0.89154 | 0.0018 |
| 4 | 0.05125 | 0.02664 | 0.05773 | 0.58162 | 0.76100 | 0.0044 |
| 5 | 0.05107 | 0.02614 | 0.05287 | 0.48540 | 0.65852 | 0.0041 |
| 6 | 0.05101 | 0.02097 | 0.04771 | 0.23016 | 0.42191 | 0.0035 |

Table 3. $e(x,y)$ and $e_{min}$ of Example 2 for some valus of $J$.

| $(x,y)$ | $J$ | *Method* | $\bar{e}$ |
|---|---|---|---|
| $(0,0.24)$ | 2 | HWFs | 0.092314 |
| | | BPFs | 0.089919 |
| | | Current | 0.085557 |
| $(0.17,0.71)$ | | HWFs | 0.105588 |
| | | BPFs | 0.096901 |
| | | Current | 0.096911 |
| $(0,0.24)$ | 4 | HWFs | 0.080441 |
| | | BPFs | 0.071561 |
| | | Current | 0.051252 |
| $(0.17,0.71)$ | | HWFs | 0.601480 |
| | | BPFs | 0.060133 |
| | | Current | 0.057737 |

Table 4. Comparison of numerical results of current method with other methods in $J = 2,4$ for Example 5.2.

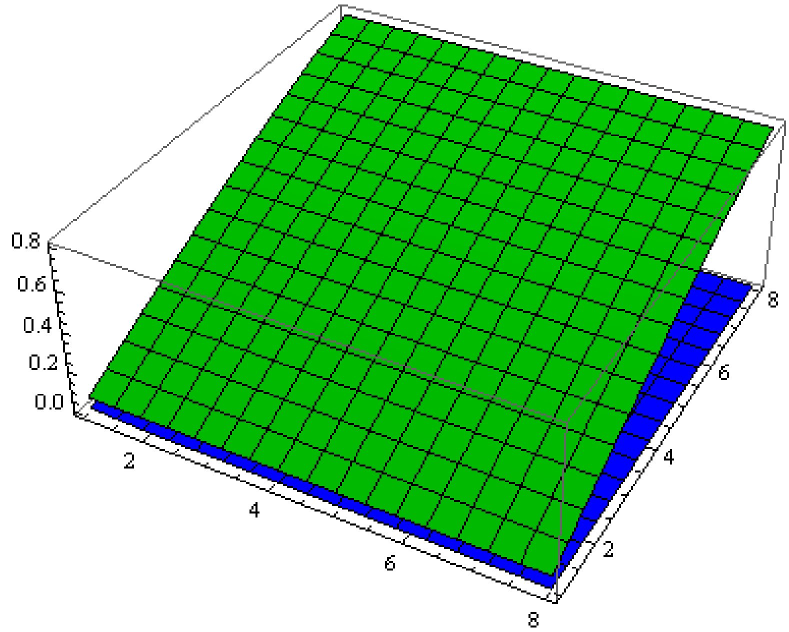


Figure 2. Exact and approximate solution ($J = 3$) for Example 5.2.

**Example 5.3.** *We consider*

$$g(x,y) = cos(x^2+y^2) - \frac{0.124}{\sqrt{x^2+y2+1}} - \frac{xlog(y+1)}{4}\Big[1 - Cos(x^2) - Cos(y^2) + (1-x^2y^2)cos(x^2+y^2) - x^2sin(x^2) - y^2sin(y^2) + (x^2+y^2)sin(x^2+y^2)\Big] + \int_0^1\int_0^1 \frac{st}{\sqrt{x^2+y2+1}}g(s,t)dsdt - \int_0^y\int_0^x xLog(y+1)s^3t^3g(s,t)dsdt,$$

*with the exact solution*

$$g(x,y) = Cos(x^2+y^2).$$

*In Table 5, $e(x,y)$ and $e_{min}$ for the arbitrary points are computed for the present method in the different values of $J$. According to Table 5, by applying this method when $J$ increases, $e(x,y)$ and $e_{min}$ decrease. You can see the 3D graphs of this example for $J = 3$ in Fig.3. Also in Table 6, the comparison of the computed results by the present method and the HWFs [18] and the BPFs [17] methods for Example 5.3 are shown. We see that the error in this method, compared to other methods is smaller.*
*In all three examples presnted in this article according to Tables 1, 3 and 5, we see that the rate of convergence increases when $J$ increases.*

| $J$ | $e(0,0.32)$ | $e(0.32,0.45)$ | $e(0.51,0.51)$ | $e(0.51,0.51)$ | $e(0.81,0.92)$ | $e_{min}$ |
|---|---|---|---|---|---|---|
| 1 | 0.10481 | 0.13153 | 0.20872 | 0.34104 | 0.78015 | 0.04495 |
| 2 | 0.10057 | 0.13083 | 0.20522 | 0.31743 | 0.74472 | 0.03579 |
| 3 | 0.08376 | 0.08151 | 0.12044 | 0.28807 | 0.62240 | 0.00854 |
| 4 | 0.00266 | 0.01827 | 0.10550 | 0.25381 | 0.51860 | 0.00029 |
| 5 | 0.00034 | 0.01124 | 0.04517 | 0.15041 | 0.42011 | 0.00017 |
| 6 | 0.00001 | 0.00265 | 0.03661 | 0.15008 | 0.26433 | 0.00000 |

Table 5. $e(x,y)$ and $e_{min}$ of Example 3 for some valus of $J$.

| $(x,y)$ | $J$ | *Method* | $\bar{e}$ |
|---|---|---|---|
| $(0,0.32)$ | 2 | HWFs | 0.122541 |
| | | BPFs | 0.115611 |
| | | Current | 0.104812 |
| $(0.26,0.83)$ | | HWFs | 0.314056 |
| | | BPFs | 0.305142 |
| | | Current | 0.322571 |
| $(0,0.32)$ | 4 | HWFs | 0.020474 |
| | | BPFs | 0.015991 |
| | | Current | 0.00266 |
| $(0.26,0.83)$ | | HWFs | 0.103466 |
| | | BPFs | 0.098497 |
| | | Current | 0.167343 |

Table 6. Comparison of numerical results of current method with other methods in $J = 2,4$ for Example 5.3.

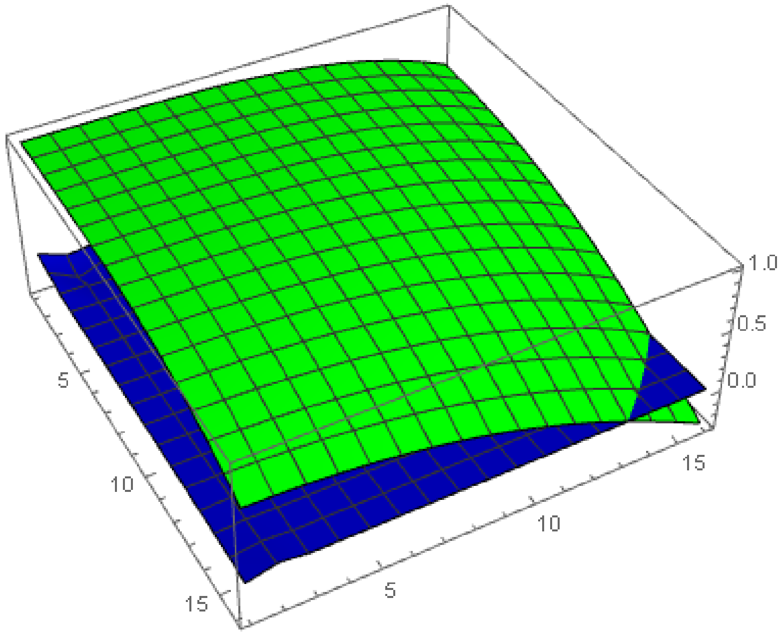


Figure 3. Exact and approximate solution ($J = 3$) for Example 5.3

## 6 Conclusion

In this paper, using the HWFs and their relations to the BPFs, a new computational method is proposed to approximate a solution of Eq. (1). The convergence analysis and the examples confirm that the method is highly accurate and sometimes leads to the exact solution. While increasing the value of $J$ theoretically improves the accuracy of the method, it results in larger linear systems of size $m_2 x m_2$. Solving these systems can be computationally expensive, especially for large values of $m_2$. Finally, this method can be improved to be more accurate by using other numerical methods such as the hybrid Hat functions and the BPFs. Mathematica has been used for computations in this paper.

## Funding

This research received no external funding.

## Data Availability Statement

Data is contained within the article.

**Acknowledgement**

The authors would like to thank the referees for their helpful comments.

**Conflicts of Interests**

The authors declare that they have no conflicts of interest regarding the publication of this article.

**References**

[1] F. Mohammadi, Haar wavelets approach for solving multidimensional stochastic Ito-Volterra integral equations, Applied Mathematics E-Notes 15 (2015) 80-96.https://www.math.nthu.edu.tw/amen/2015/AMEN(140902).pdf
[2] Z.H. Jiang, W. Schaufelberger, Block pulse functions and their applications in control systems, Springer-Verlag, 1992.https://doi.org/10.1007/bfb0009162
[3] W. Rudin, Principles of mathematical analysis, McGraw-Hill Publishing Company Ltd., 1976. https://doi.org/10.1017/s002555720005333x
[4] F. Keinert, Wavelets and Multiwavelets, A Crc Press Company, Boca Raton, London, New York, Washington DC, 2004. https://doi.org/10.1201/9780203011591
[5] K. Maleknejad, Z. Jafari-Behbahani, Application of two-dimensional triangular functions for solving nonlinear class of mixed Volterra-Fredholm integral equations, Math. Comp. Mode. 55 (2012) 1833-1844. https://doi.org/10.1016/j.mcm.2011.11.041
[6] E. Babolian, K. Maleknejad, M. Roodaki, H. Almasieh, Two dimensional triangular functions and their applications to nonlinear 2d Volterra-Fredholm equations, Comp. Math. App. 60 (2012) 1711-1722. https://doi.org/10.1016/j.camwa.2010.07.002
[7] F. Hosseini Shekarabi, K. Maleknejad, R. Ezzati, Application of two-dimensional Bernstein polynomials for solving mixed Volterra-Fredholm integral equations, African Mathematical Union and Springer-Verlag Berlin Heidelberg, 2014. https://doi.org/10.1007/s13370-014-0283-6
[8] D. Darshana, B. Jayanta, On the solution of nonlinear nonlocal Volterra-Fredholm type hybrid fractional differential equation, Indian Journal of Pure and Applied Mathematics (2023) 1–12. https://doi.org/10.1007/s13226-023-00462-7
[9] A. R. Yaghoobnia, R. Ezzati, Numerical solution of Volterra–Fredholm integral equation systems by operational matrices of integration based on Bernstein multi-scaling polynomials, Comp. and Appl. Math. 41 (2022) 324. https://doi.org/10.1007/s40314-022-02036-5
[10] K. Parand, H. Yari, M. Delkhosh, Solving two-dimensional integral equations of the second kind on non-rectangular domains with error estimate, Engineering with Computers 36 (2020) 725–739. https://doi.org/10.1007/s00366-019-00727-y
[11] P. Assari, M. Dehghan, The approximate solution of nonlinear Volterra integral equations of the second kind using radial basis functions, Appl. Numer. Math. 131 (2018) 140–157. https://doi.org/10.1016/j.apnum.2018.05.001
[12] W. Xie, F. R. Lin, A fast numerical solution method for two dimensional Fredholm integral equations of the second kind, App. Num. Math. 59 (2009) 1709-1719. https://doi.org/10.1016/j.apnum.2009.01.009
[13] S. Bazm, E. Babolian, Numerical solution of nonlinear two-dimensional Fredholm integral equations of the second kind using Gauss product quadrature rules, Commun. Nonlinear Sci. Numer. Simult. 17 (2012) 1215–1223. https://doi.org/10.1016/j.cnsns.2011.08.017
[14] S. Nemati, P. Lima, Y. Ordokhani, Numerical solution of a class of two-dimensional nonlinear Volterra integral equations using legender polynomials, J. Comp. Appl. Math. 242 (2013) 53–69. https://doi.org/10.1016/j.cam.2012.10.021
[15] A. Tari, M. Rahimi, S. Shahmorad, F. Talati, Solving a class of two-dimensional linear and nonlinear

Volterra integral equations by the differential transform method, J. Comp. Appl. Math. 228 (2009) 70–76. https://doi.org/10.1016/j.cam.2008.08.038

[16] P. Assari, H. Adibi, M. Dehghal, A meshless method for solving nonlinear two-dimensional integral equations of the second kind on non-rectangular domains using radial basis functions with error analysis, J. Comp. Appl. Math. 239 (2013) 72–92. https://doi.org/10.1016/j.cam.2012.09.010

[17] M. Fallahpour, M. Khodabin, K. Maleknejad, Theoretical error analysis and validation in numerical solution of two-dimensional linear stochastic Volterra-Fredholm integral equation by applying the block-pulse functions, Cog. Math. 4 (2017) 1296750. https://doi.org/10.1080/23311835.2017.1296750

[18] M. Fallahpour, M. Khodabin, K. Maleknejad, Theoretical error analysis of solution for two-dimensional stochastic Volterra integral equations by Haar wavelet, Int. J. Appl. Comput. Math (2019) 1–13. https://doi.org/10.1007/s40819-019-0739-3

**Citation:** M. Fallahpour, R. Ezzati, E. Hashemizadeh, A combined efficient method for approximate two-dimensional integral equations, J. Disc. Math. Appl. 9(4) (2024) 269–287.

**https://doi.org/10.22061/jdma.2024.11175.1088**